第 34 卷第 11 期
2018 年 11 月

无 机 化 学 学 报
CHINESE JOURNAL OF INORGANIC CHEMISTRY

Vol.34 No.11
2041-2048

# 染料敏化太阳能电池对电极 $La_2Mo_2O_7$ 复合 MWCNTs 非 Pt 催化剂的制备与性能

武克忠　赵佳静　熊元元　阮　北　武明星*

(河北师范大学化学与材料科学学院,河北省无机纳米重点实验室,石家庄　050024)

**摘要**：通过高温固相法对醋酸镧($C_6H_9O_6La\cdot xH_2O$)与高钼酸铵($(NH_4)_6Mo_7O_{24}\cdot 4H_2O$)在一定条件下热解制备非 Pt 催化剂 $La_2Mo_2O_7$ ($La_2O_3$-2$MoO_2$)。进一步采用 2 种方法将 $La_2Mo_2O_7$ 与多壁碳纳米管(MWCNTs)进行复合,一种是将 $La_2Mo_2O_7$ 喷涂到 MWCNTs 表层之上得到 $La_2Mo_2O_7$/MWCNTs,另一种是将两者均匀混合掺杂得到 $La_2Mo_2O_7$@MWCNTs,再将上述 2 种复合材料应用于染料敏化太阳能电池对电极进行相应研究。通过扫描电子显微镜(SEM)表征了复合催化材料的微观形貌,X 射线衍射(XRD)确定了微观结构。采用电流密度–光电压曲线、循环伏安,交流阻抗以及塔菲尔极化分析了材料的光电性能。实验结果表明在电解液 $I_3^-/I^-$中,基于 $La_2Mo_2O_7$/MWCNTs 与 $La_2Mo_2O_7$@MWCNTs 的对电极，相同的条件下在光电池中获得的光电转换效率分别为 6.09%和 4.84%,明显高于 MWCNTs 的 3.94%和 $La_2Mo_2O_7$ 的 0.87%。电极性能的提高可归因于 $La_2Mo_2O_7$ 复合催化剂相对大的比表面积和高导电性。

**关键词**：染料敏化太阳能电池；能量转换效率；对电极；钼酸铵；复合物

**中图分类号**：O613.2　　**文献标识码**：A　　**文章编号**：1001-4861(2018)11-2041-08

**DOI**:10.11862/CJIC.2018.249

# Synthesis and Performance of $La_2Mo_2O_7$ with MWCNTs Composite Materials as Pt-Free Counter Electrodes for Dye Sensitized Solar Cells

WU Ke-Zhong　ZHAO Jia-Jing　XIONG Yuan-Yuan　RUAN Bei　WU Ming-Xing*

(*Key Laboratory of Inorganic Nano-Materials of Hebei Province, Department of Chemistry and Material Science, Hebei Normal University, Shijiazhuang* 050024, *China*)

**Abstract:** A Pt-free counter electrode (CE) composed of $La_2Mo_2O_7$ ($La_2O_3$-2$MoO_2$) was successfully synthesized via the simple pyrolysis of lanthanum acetate ($C_6H_9O_6La\cdot xH_2O$) and hexaammonium heptamolybdate tetrahydrate ($(NH_4)_6Mo_7O_{24}\cdot 4H_2O$) in a high-temperature solid-state reaction. Also, $La_2Mo_2O_7$ and multiwall carbon nanotubes (MWCNTs) are combined using two methods. $La_2Mo_2O_7$/MWCNTs was prepared by spray-coating $La_2Mo_2O_7$ over the surface of MWCNTs, and $La_2Mo_2O_7$@MWCNTs was synthesized by doping $La_2Mo_2O_7$ into MWCNTs. The two types of composite materials were further used as Pt-free catalytic material in CEs in dye sensitized solar cells (DSSCs). The morphology and microstructure of $La_2Mo_2O_7$/MWCNTs and $La_2Mo_2O_7$@MWCNTs were determined using scanning electron microscopy and X-ray diffraction. The electrochemical performance of the $La_2Mo_2O_7$/MWCNTs and $La_2Mo_2O_7$@MWCNTs composite catalysts for CEs was determined using photocurrent-voltage measurements, cyclic voltammetry, electrochemical impedance spectroscopy, and Tafel polarization in encapsulation of DSSCs batteries. The experimental results show that power conversion efficiencies of 6.09% and 4.84% were obtained for $La_2Mo_2O_7$/MWCNTs and $La_2Mo_2O_7$@MWCNTs, respectively, as CEs toward the reduction

收稿日期:2018-03-21。收修改稿日期:2018-09-01。

国家自然科学基金(No.21473048,21303039),河北自然科学基金(No.B2015205163,B2016205161),河北省科技厅计划项目(No.16211117)和河北教育厅计划项目(No.QN2017087)资助。

*通信联系人。E-mail:sc05019017@163.com

of $I_3^-/I^-$ ions, and these values are superior to those of MWCNTs (3.94%) and the $La_2Mo_2O_7$ (0.87%) electrode under the same conditions. The enhanced electrode performance was attributed to the relatively larger surface area and higher conductivity of the $La_2Mo_2O_7$/MWCNTs composite catalysts.

**Keywords:** dye-sensitized solar cell; power conversion efficiency; counter electrode; molybdenum acid lanthanum; composite material

## 0 Introduction

Dye sensitized solar cells (DSSCs) directly convert solar energy into electricity to improve energy efficiency and protect the environment[1-3]. DSSCs consist of a transparent photoanode, electrolyte, and a counter electrode (CE). The CE is an important component of DSSCs and plays an important role in collecting electrons from an external circuit and in catalyzing the regeneration of the redox couple at the CE/electrolyte interface[4-5]. Generally, Pt is widely used as a catalytic material on CEs because of its high catalytic activity and high efficiency[6-8]. However, Pt is not only expensive and rare but can also be readily corroded by the $I_3^-/I^-$ electrolyte. Development of Pt-free catalysts is considered to be one of the crucial steps toward improved energy conversion efficiency and low-cost alternatives of DSSCs.

A significant amount of Pt-free catalytic materials for the CE in DSSCs has been reported, and these materials have included carbon materials (activated carbon, multiwall carbon nanotubes (MWCNTs), graphite, nanotubes, graphene, and $C_{60}$)[9-12], conducting and doped polymers (polypyrrole (PPy), polyaniline (PAn), polythiophene (PTh), polyphenylene (PPP), and poly-(3,4-ethylene dioxythiophene) (PEDOT))[13-15], and transition metal compounds (oxides, nitrides, carbides, sulfides, and selenides)[16-25]. Among the transition metal compounds, La-Mo compounds and their corresponding composites might be essential in various electrochemical devices because of their great flexibility in structure and morphology, convenience in synthesis, and high electrocatalytic activity toward the electrolyte[26]. Wu et al.[27] synthesized molybdenum carbide microspheres ($Mo_2C$-Ms) and nanorods ($Mo_2C$-Nr) as CE catalysts. The DSSCs resulted in power conversion efficiencies (PCEs) of 5.50% and 4.86% for $Mo_2C$-Ms and $Mo_2C$-Nr, respectively. The performance of single catalysts can be further improved through the use of conductive carbon and carbon derivative materials. Previously, Jin et al.[28] successfully synthesized nanocomposites of the perovskite-phase $La_{0.65}Sr_{0.35}MnO_3$ with reduced graphene oxide (LSMO@RGO). Areerob et al.[29] fabricated DSSCs using La/$TiO_2$-graphene nanocomposite CEs and their DSSCs yielded a PCE of 6.75%. La/$TiO_2$-graphene CEs exhibited efficient electrocatalytic ability because the catalytic La particles were uniformly distributed on the surface of graphene.

In our preliminary experiments, we have synthesized a series of solid solution and intermediate compounds of $La_2O_3$-$MoO_3$, with the different stoichiometric ratios from 0∶1 to 1∶0, according to the phase diagram of $La_2O_3$-$MoO_3$[30]. The performance of $La_2Mo_2O_7$ as a CE catalyst is superior to other materials for the reduction of $I_3^-/I^-$ in DSSCs. Herein, we combined $La_2Mo_2O_7$ with MWCNTs to synthesize $La_2Mo_2O_7$/MWCNTs and $La_2Mo_2O_7$@MWCNTs electrodes to improve the performance of DSSCs. Carbon composites have attracted research attention for enhancing the value of products and for reducing production costs, which has become increasingly important. MWCNTs is a kind of carbon material that has a significant amount of void spaces, a large specific surface area, and acts as a carrier and catalyst[31]. $La_2Mo_2O_7$/MWCNTs and $La_2Mo_2O_7$@MWCNTs were investigated in iodine electrolyte, and they exhibited high PCEs in DSSCs. The composites have both the increased active surface area of the MWCNTs and the coupling effects between $La_2Mo_2O_7$ and MWCNTs[19]. $La_2Mo_2O_7$/MWCNTs composite catalytic materials exhibited high electrocatalytic activity and low charge transfer resistance.

## 1 Experimental

### 1.1 Synthesis of the composites

Lanthanum acetate hydrate ($La(CH_3COO)_3 \cdot xH_2O$, 99.9%, molecular weight: 316.04) was supplied by Aladdin, Shanghai. Hexaammonium heptamolybdate tetrahydrate ($(NH_4)_6Mo_7O_{24} \cdot 4H_2O$, ≥99.0%, molecular weight: 1 235.86) was supplied by Sinopharm Chemical Reagent Co., Ltd. MWCNTs was supplied by Aladdin, Shanghai. All reagents and solvents were analytical grade and were used without further purification. La $(CH_3COO)_3 \cdot xH_2O$ and $((NH_4)_6Mo_7O_{24} \cdot 4H_2O)$ were mixed according to their stoichiometric ratio and ground in an agate mortar with 3 mL of ethanol. The mixture was then placed in an oven to dry at 150 ℃ and pressed at 8 MPa into pellets that had a 10 mm diameter. Then, $La_2Mo_2O_7$ ($La_2O_3$-$2MoO_2$) was obtained from the solid precursor via a high-temperature solid phase reaction at 800 ℃ for 8 h in air. The synthesis of $La_2Mo_2O_7$@MWCNTs was performed by doping 0.125 0 g of $La_2Mo_2O_7$ on 0.025 0 g of MWCNTs in isopropanol solvent using ultrasonic dispersion for 15 min. The mixture pastes of $La_2Mo_2O_7$@MWCNTs were obtained for $La_2Mo_2O_7$ and MWCNTs with mass ratios of 5:1.

### 1.2 Cell fabrication

Pt, pure $La_2Mo_2O_7$, $La_2Mo_2O_7$@MWCNTs and $La_2Mo_2O_7$/MWCNTs composites were used as CEs and prepared as follows: An FTO glass substrate piece was cleaned with distilled water, then cleaned with a mixture of ethanol and acetone in an ultrasonic bath, and dried under a hot dryer. Then, 100 mg of the prepared $La_2Mo_2O_7$, $La_2Mo_2O_7$@MWCNTs and the purchased MWCNTs were respectively dispersed in 2 mL of isopropanol. These mixture pastes were obtained via ball-milling for 50 min and directly sprayed on each FTO glass using an airbrush. The thickness of the electrode was about (12±1) μm. The preparation of $La_2Mo_2O_7$/MWCNTs was first sprayed with 6 μm of MWCNTs on the FTO glass and then sprayed with 6 μm of $La_2Mo_2O_7$ onto the surface of the MWCNTs. $La_2Mo_2O_7$ and MWCNTs show upper and lower layers on the FTO glass. Followed by next step, the FTO glass, which was coated with active material paste of $La_2Mo_2O_7$, $La_2Mo_2O_7$@MWCNTs, MWCNTs and $La_2Mo_2O_7$/MWCNTs, was sintered at 500 ℃ under $N_2$ flow for 30 min, and the CEs were obtained. Preparation of the Pt CE was carried out using a chemical reduction method. A mass fraction of 5% chloroplatinic acid isopropanol was sprayed onto the ITO substrate and dried at 120 ℃ for 1 h. Then, the ITO substrate was rapidly immersed in an aqueous solution of 30 $mmol \cdot L^{-1}$ $NaBH_4$ for 3 min. The ITO substrate was then removed and rinsed with water and absolute ethanol and dried at 120 ℃ for 1 h. The photoanode used in the DSSCs was a 12-mm thick $TiO_2$ film sensitized with N719 dye. The electrolyte $I_3^-$/$I^-$ contained 0.1 $mol \cdot L^{-1}$ LiI, 0.6 $mol \cdot L^{-1}$ 1-propyl-3-methylimidazolium iodide, 0.07 $mol \cdot L^{-1}$ $I_2$, 0.5 $mol \cdot L^{-1}$ 4-*tert*-butyl pyridine, and 0.1 $mol \cdot L^{-1}$ guanidinium thiocyanate in 3-methoxypropionitrile (MPN). The active area of the electrode was about 0.4 cm×0.4 cm. For electrochemical measurements, the symmetrical cell had a sandwich configuration and was fabricated with two identical CEs clipping the electrolyte together using hot-melt surlyn film.

### 1.3 Measurements

The XRD pattern of $La_2Mo_2O_7$, MWCNTs and $La_2Mo_2O_7$@MWCNTs material powders was taken by a D8 Bruker X-ray diffractometer ($\lambda$=0.154 nm) using Cu $K\alpha$ radiation (Ni filter) at $2° \cdot min^{-1}$ with $2\theta$ ranging from 10° to 70°. The voltage is 40 kV and the current is 40 mA. Scanning electron microscopy (SEM) was performed with an S-4800 SEM instrument (Hitachi, Japan) at an accelera-tion voltage of 3 kV. The cyclic voltammetry (CV), electrochemical impedance spectroscopy (EIS), and Tafel polarization tests were performed using a CHI 660E (SHANGHAI, CHEN HUA) electrochemical analyzer. The CV experiments were carried out in a two-compartment glass cell with a three-electrode configuration at 25 ℃ in an acetonitrile solution containing 1 $mmol \cdot L^{-1}$ iodine ($I_2$), 0.1 $mol \cdot L^{-1}$ $LiClO_4$ (lithium perchlorate), and 10 $mmol \cdot L^{-1}$ LiI (lithium iodate). The as-fabricated CEs acted as the working electrode, the Pt sheet (4 $cm^2$) as the counter electrode, and a saturated calomel

electrode (SCE) as the reference electrode. All potentials were presented on the SCE scale. EIS was carried out in the frequency range of 0.01 ~$10^5$ Hz at 0 V bias voltage with perturbation amplitude of 5 mV in the dark. Tafel polarization was measured at a scan rate of 10 mV·$s^{-1}$ from −0.7 to 0.7 V. The assembled DSSCs were illuminated under AM 1.5 illumination ($I$=100 mW·$cm^{-2}$, PEC-L01, Peccell, Yokohama, Japan) with a digital source meter (Keithley 2601, Cleveland, OH).

## 2 Results and discussion

### 2.1 Characterization of the as-prepared composites

The XRD patterns for MWCNTs, $La_2Mo_2O_7$, and $La_2Mo_2O_7$@MWCNTs were recorded at room temperature and are presented in Fig.1. In the diffraction pattern of the powder sample, the most intense diffraction peak values of $La_2Mo_2O_7$ are at 15.96°, 27.65°, 28.14°, 31.06°, 33.50°, 39.83°, 46.49°, 48.76°, 52.90°, 55.66°, and 64.35°, which could be well identified as (210), (310), (011), (111), (120), (301), (002), (610), (421), (430), and (422) and matched well with pristine $La_2Mo_2O_7$ (PDF No.84-1234). Fig.1 shows a typical XRD pattern of MWCNTs subjected to $N_2$ annealing at 500 ℃. It is known that MWCNTs have a strong and sharp characteristic peak at $2\theta$=26.59°, and this peak is attributed to diffraction of the single carbon atom. The diffraction patterns of $La_2Mo_2O_7$@MWCNTs are similar to that of pure $La_2Mo_2O_7$. The amorphous peak of MWCNTs is relatively weak in the $La_2Mo_2O_7$@MWCNTs sample, and this result indicates that MWCNTs was barely physically combined with $La_2Mo_2O_7$ as catalyst carriers.

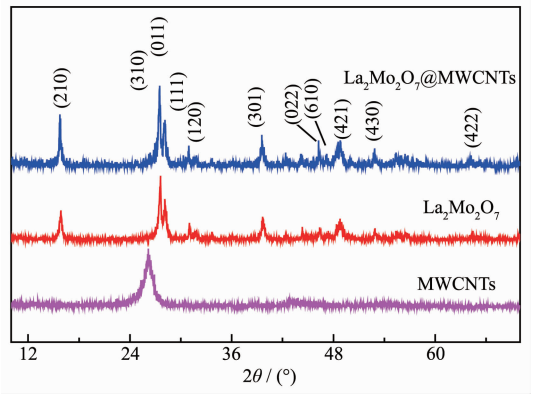


Fig.1 XRD patterns of the prepared MWCNTs, $La_2Mo_2O_7$ and $La_2Mo_2O_7$@MWCNTs

Fig.2 shows the morphologies of the MWCNTs, $La_2Mo_2O_7$, $La_2Mo_2O_7$@MWCNTs, and $La_2Mo_2O_7$/MWCNTs. The MWCNTs had attained a clear shape of nanofibers with smooth, uniform and beads-free

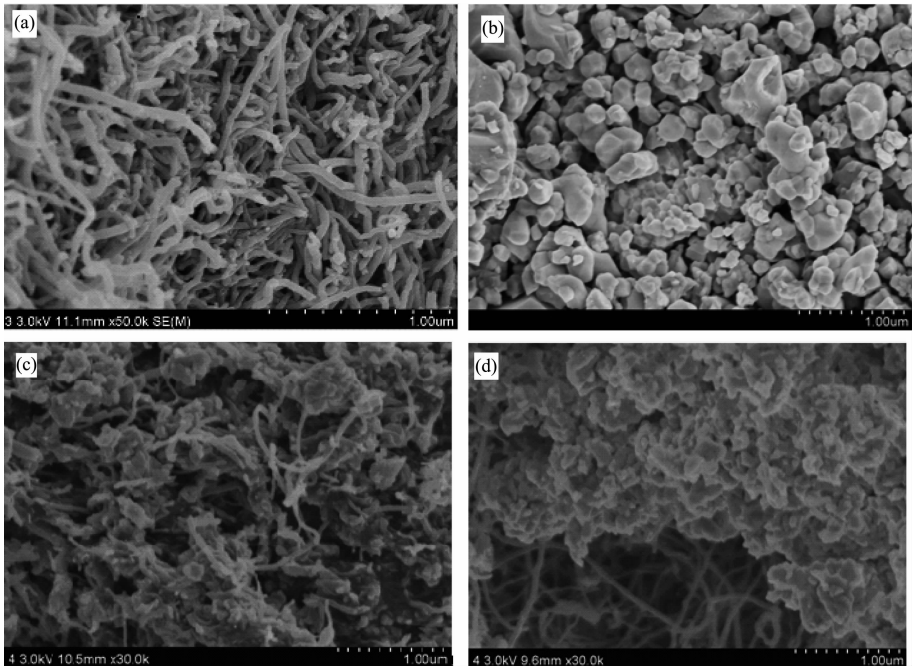


Fig.2 SEM images of the prepared MWCNTs (a), $La_2Mo_2O_7$ (b), $La_2Mo_2O_7$@MWCNTs (c) and $La_2Mo_2O_7$/MWCNTs (d)

surface (Fig.2(a)). There are some void spaces, observed around the MWCNTs. The particle size of $La_2Mo_2O_7$ is the smallest and more evenly distributed, as seen in Fig.2(b). Fig.2(c) shows that $La_2Mo_2O_7$ was fully combined with MWCNTs to construct $La_2Mo_2O_7$@MWCNTs; Fig.2(d) shows sectional view morphology that the small area $La_2Mo_2O_7$ coating was scraped away from the surface of the $La_2Mo_2O_7$/MWCNTs electrode using a blade. The $La_2Mo_2O_7$/MWCNTs electrode presents upper and lower layers. The intact part of the electrode $La_2Mo_2O_7$ is uniformly distributed over the MWCNTs.

## 2.2 Application of the as-prepared composites

Fig.3 presents photocurrent density-voltage (*J-V*) curves of the DSSCs using CEs based on Pt, MWCNTs, $La_2Mo_2O_7$, $La_2Mo_2O_7$/MWCNTs, and $La_2Mo_2O_7$@MWCNTs. The photovoltaic parameters are presented in Table 1, where $V_{oc}$ presents the open-circuit voltage. Fig.3 shows that PCEs of 6.09% and 4.84% were obtained for $La_2Mo_2O_7$/MWCNTs and $La_2Mo_2O_7$@MWCNTs, respectively, and these values were superior to the PCEs of Pt (4.54%), MWCNTs (3.94%), and $La_2Mo_2O_7$ (0.87%) CE-based DSSCs. The short-circuit current density ($J_{SC}$) of the four materials were in the order of: $La_2Mo_2O_7$/MWCNTs (12.19 mA·cm$^{-2}$) > $La_2Mo_2O_7$@MWCNTs (10.88 mA·cm$^{-2}$) > MWCNTs (9.75 mA·cm$^{-2}$) > $La_2Mo_2O_7$ (8.88 mA·cm$^{-2}$). The significantly enhanced $J_{SC}$ values contribute to the improved performance of the DSSCs and reveal that the rate of pore recovery at the $La_2Mo_2O_7$@MWCNTs and $La_2Mo_2O_7$/MWCNTs electrode-electrolyte interface were faster than that at the electrode-electrolyte interface of the other CEs. Furthermore, fill factor (FF) values of the $La_2Mo_2O_7$/MWCNTs and $La_2Mo_2O_7$@MWCNTs cathodes were as high as 0.64 and 0.63, which were higher than the FF of 0.13 indicated by the $La_2Mo_2O_7$ CE-based DSSC. FF mainly reflects the internal resistance of the electrode/electrolyte in a cell. Thus, the higher $J_{SC}$ and FF values for the four materials used as CEs are ascribed to the considerable enhancement in charge transfer at the CE/electrolyte interface and to catalytic ability, which lowers the internal resistances, the concentration gradients in the electrolyte, and the recombination rates[32]. The high catalytic activity of each of the $La_2Mo_2O_7$@MWCNTs and $La_2Mo_2O_7$/MWCNTs used in the DSSCs could be because of the MWCNTs increased catalytic surface area of the electrode films.

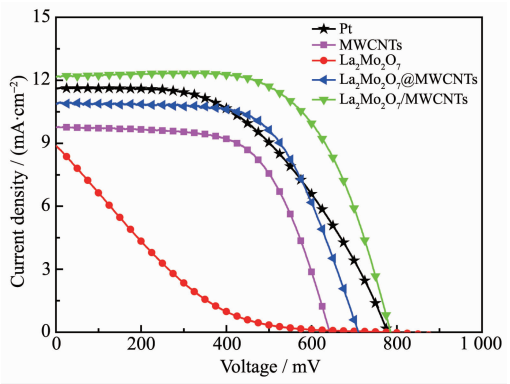


Fig.3 *J-V* characteristics of DSSCs with different samples as CEs under a light intensity of 100 mW·cm$^{-2}$

## 2.3 Electrocatalytic process of electrodes

The CV measurements were conducted at a scan rate of 20 mV·s$^{-1}$ to determine the electrocatalytic kinetics of five materials toward the reduction couple of $I_3^-/I^-$ in 3-methoxypropionitrile solution, which consisted of 1 mmol·L$^{-1}$ $I_2$, 10 mmol·L$^{-1}$ LiI and 0.1 mol·L$^{-1}$ $LiClO_4$. The CV curves are presented in Fig. 4. It is noteworthy that two oxidation-reduction couples were observed in the CV curves of all five samples.

The reduction peaks in the negative potential could be associated with the reaction: $I_3^- + 2e^- \rightarrow 3I^-$; the oxidation peaks in the negative potential

**Table 1 Photovoltaic parameters for the DSSCs assembled with various CEs**

| CE | $V_{oc}$ / mV | $J_{SC}$ / (mA·cm$^{-2}$) | FF | PCE / % |
|---|---|---|---|---|
| Pt | 779 | 11.63 | 0.50 | 4.54 |
| MWCNTs | 643 | 9.75 | 0.63 | 3.94 |
| $La_2Mo_2O_7$ | 777 | 8.88 | 0.13 | 0.87 |
| $La_2Mo_2O_7$@MWCNTs | 710 | 10.88 | 0.63 | 4.84 |
| $La_2Mo_2O_7$/MWCNTs | 786 | 12.19 | 0.64 | 6.09 |

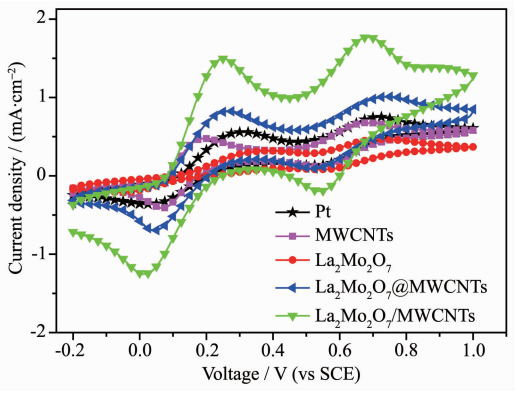


Fig.4 CV curves of various CE electrodes for the $I^-/I_3^-$ electrolyte

correspond to the reaction: $3I^- \longrightarrow I_3^- + 2e^-$ [33]. Two main parameters from the CV curve demonstrated the entire electrocatalytic abilities, and these parameters were the peak-to-peak separation ($\Delta E_p$) and the cathodic peak current density ($I_P$) at more negative potential. In the case of composites, the $\Delta E_p$ values of $La_2Mo_2O_7$/MWCNTs and $La_2Mo_2O_7$@MWCNTs were 0.222 and 0.237 V, respectively. The values of $\Delta E_p$ are lower than that of the CE assembled with the $La_2Mo_2O_7$ (0.377 V) electrode, and this indicates the enhanced electrocatalytic activity and reversibility of the $La_2Mo_2O_7$/MWCNTs and $La_2Mo_2O_7$@MWCNTs CEs. The $\Delta E_p$ value is attributed to the redox ability of the counter electrode to electric pair in electrolytes. The lower $\Delta E_p$ value corresponds to the higher redox capability of CE for $I_3^-/I^-$. The $I_P$ values from the CV profile also demonstrated the electrocatalytic activity of CE. The $I_P$ values of the $La_2Mo_2O_7$/MWCNTs (1.255 $mA \cdot cm^{-2}$) and $La_2Mo_2O_7$@MWCNTs (0.702 3 $mA \cdot cm^{-2}$) composite CEs are higher than that of the CEs with the $La_2Mo_2O_7$ (0.211 0 $mA \cdot cm^{-2}$), MWCNT$_S$ (0.412 0 $mA \cdot cm^{-2}$), and Pt (0.363 0 $mA \cdot cm^{-2}$) electrodes. The higher $I_P$ values indicated the excellent electrocatalytic activity of the two $La_2Mo_2O_7$-MWCNTs composites, which are promising as Pt-free efficient CEs in DSSCs. Moreover, the catalytic reaction is a kinetic process, which is associated with the electron transfer rate constant and the number of active sites. The ntegral area of the negative redox peak for each of the two composite electrodes was bigger than that for $La_2Mo_2O_7$ ($La_2O_3$-2$MoO_2$) and MWCNTs, which indicateed that the $La_2Mo_2O_7$-MWCNTs composite structure provides more catalytic reaction sites than the $La_2Mo_2O_7$ and MWCNTs CEs.

EIS was carried out to assess the electrical conductivity and electrochemical catalytic activities of the CEs. Fig.5 presents the Nyquist plots of the symmetric cells using different materials as the CEs. The charge transfer resistance ($R_{ct}$) of the CE can be taken as half the value of the real semicircles in the high-frequency region. The $R_{ct}$ values of Pt, MWCNTs, $La_2Mo_2O_7$, and the $La_2Mo_2O_7$@MWCNTs and $La_2Mo_2O_7$/MWCNTs composites were 54.0, 634.4, 2 007.3, 328.4, and 262.2 Ω, respectively. The data indicate that the $R_{ct}$ value of the $La_2Mo_2O_7$ electrode is much larger and the $La_2Mo_2O_7$/MWCNTs composite electrode is smaller than those of the other CE-based cells. The $La_2Mo_2O_7$/MWCNTs and $La_2Mo_2O_7$@MWCNTs CEs demonstrated better redox capacity and high electrocatalytic ability than the $La_2Mo_2O_7$ and MWCNTs CE. This is attributed to the lower conductivity of the composites and the accelerated high electron transmission at the CE/electrolyte interface, which thus result in higher $J_{sc}$ and FF.

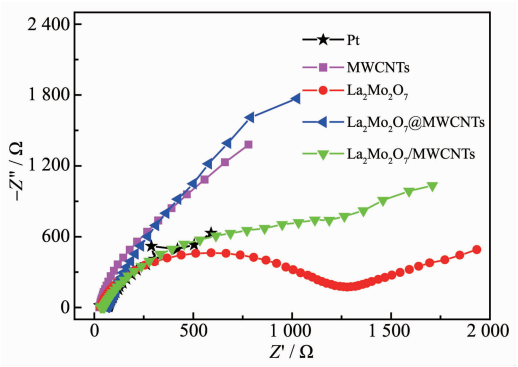


Fig.5 Nyquist plots for symmetrical cells based on various CEs

Tafel polarization curves were recorded at a scan rate of 10 $mV \cdot s^{-1}$ from −0.7 to 0.7 V to estimate the electrocatalytic activity of different CEs for $I_3^-$ reduction. The exchange current density ($J_0$) of DSSCs can be regarded as the intercept of the extrapolated linear region of the anodic and cathodic branches when the potential is zero. The anodic and cathodic branches of the Tafel curves for $La_2Mo_2O_7$/MWCNTs and the composite $La_2Mo_2O_7$@MWCNTs CEs show larger slopes than that for the MWCNTs and $La_2Mo_2O_7$ CEs, exhibiting a higher exchange current density ($J_0$) on

CE in Fig.6[30]. Both the $La_2Mo_2O_7$/MWCNTs and $La_2Mo_2O_7$@MWCNTs CEs demonstrated higher $J_0$ values than the $La_2Mo_2O_7$ and MWCNTs electrodes, and a maximal $J_0$ value for the $La_2Mo_2O_7$/MWCNTs CE was observed. Obviously, the order of $J_0$ is $La_2Mo_2O_7$/MWCNTs (0.416 4 mA·cm$^{-2}$) > $La_2Mo_2O_7$@MWCNTs (0.199 1 mA·cm$^{-2}$) > MWCNTs (0.158 6 mA·cm$^{-2}$) > $La_2Mo_2O_7$ (0.019 96 mA·cm$^{-2}$). This order indicates that the $La_2Mo_2O_7$/MWCNTs and $La_2Mo_2O_7$@MWCNTs composites possessed higher diffusion velocities and better electrocatalytic activities for the reduction of $I_3^-$ than the MWCNTs and $La_2Mo_2O_7$ CEs. This is consistent with the trend of the cathodic peak current shown in the CV curve. The $J_0$ value can be directly calculated using Eq.(**1**):

$$J_0=\frac{RT}{nFR_{ct}} \quad (1)$$

Where $R$ is the gas constant, $T$ is the absolute temperature (K), $n$ is the number of electrons related to the electrochemical reduction reaction in the reduction of $I_3^-$. The $J_0$ value is inversely proportional to the $R_{ct}$ value. A larger $J_0$ value indicates more electrons migrating through the CE/electrolyte interface, and this thereby indicates that the catalytic film has a faster electron transfer capability. Tafel polarization results match well with EIS and CV results. The experimental results clearly reveal that the composite of $La_2Mo_2O_7$ and MWCNTs obtained the higher charge transfer between $I_3^-$ ions and the $La_2Mo_2O_7$/MWCNTs surfaces and the rapid redox transfer reaction of $I_3^-/I^-$ in a dye-sensitized solar cell system.

The $La_2Mo_2O_7$/MWCNTs CEs demonstrated higher PCE, $J_{sc}$ and $V_{oc}$ of CEs values than that of Pt, $La_2Mo_2O_7$, $La_2Mo_2O_7$@MWCNTs and MWCNTs CEs from *J-V* curves. The maximal PCE value was obtained for $La_2Mo_2O_7$/MWCNTs composite, which was 6.09%. The CV results were in good agreement with the PCE results from *J-V* measurements. From the CV curves, $La_2Mo_2O_7$/MWCNTs had shown the lowest $\Delta E_p$ and highest $I_P$. The Tafel polarization results indicated that $La_2Mo_2O_7$/MWCNTs CEs obtained the higher $J_0$, as compared to other CEs, which indicated a higher catalytic activity of composite CEs. According to Eq. (**1**), the $R_{ct}$ was inversely proportional to $J_0$. We can deduce that $R_{ct}$ of composite CEs was higher than that of $La_2Mo_2O_7$ and MWCNTs, which is in good agreement with the experimentally measured $R_{ct}$ from EIS. Compared with $La_2Mo_2O_7$@MWCNTs, $La_2Mo_2O_7$/MWCNTs enhanced catalytic active sites, increased exchange current density and load resistance reduction at CE/electrolyte interface.

The CV, EIS, Tafel, and *J-V* characterizations demonstrated that the $La_2Mo_2O_7$/MWCNTs CEs could catalyze the regeneration of the $I_3^-/I^-$ couple, as effectively as Pt. In addition, a desirable catalyst should possess robust stability along with high catalytic activity. Thus, herein, we checked the electrochemical stability of the $La_2Mo_2O_7$/MWCNTs CEs via consecutive CV cycling (Fig.7). After 10 consecutive CV cycles, minor current density attenuation or no peak position shift was observed, this demonstrates that $La_2Mo_2O_7$/MWCNTs was stable and coexist with the $I^{3-}/I^-$ redox couples.

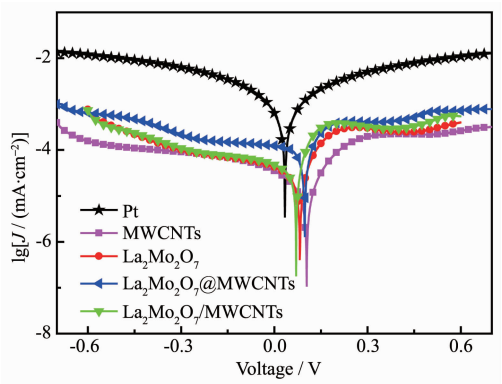


Fig.6 Tafel plots of symmetrical cells between −0.7~0.7 V with a scan rate of 10 mV·s$^{-1}$ at room temperature

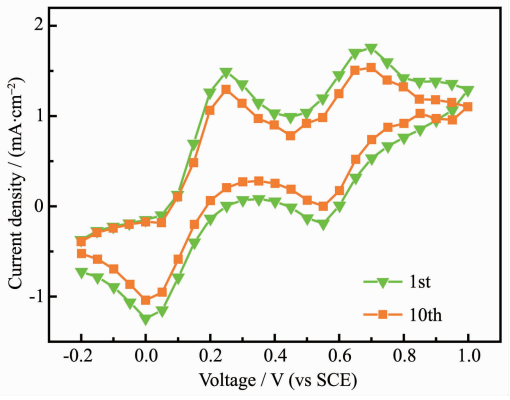


Fig.7 CVs of $La_2Mo_2O_7$/MWCNTs CE for the $I^-/I_3^-$ electrolyte 1st and 10th cycle

## 3 Conclusions

Composite materials of $La_2Mo_2O_7$ with MWCNTs were successfully synthesized using a high-temperature solid-state reaction. $La_2Mo_2O_7$ was modified on the surface of MWCNTs to synthesize $La_2Mo_2O_7$/MWCNTs and doped in MWCNTs to synthesized $La_2Mo_2O_7$@MWCNTs. Both composite materials served as Pt-free catalytic materials for CEs for efficient DSSCs. MWCNTs and $La_2Mo_2O_7$ combined to expand the surface area, increase the exchange current density of the composite materials, and reduce the load resistance at the counter electrode/electrolyte interface. MWCNTs act as both a carrier and a catalyst. Power conversion efficiency values of 6.09% and 4.84% were obtained for $La_2Mo_2O_7$/MWCNTs and $La_2Mo_2O_7$@MWCNTs, respectively, using each as a counter electrode, and these values are superior to those of Pt (4.54%), $La_2Mo_2O_7$ (0.87%), and MWCNTs (3.94%) toward the reduction of $I_3^-/I^-$ ions. Thus, after an integrated analysis of the CV, EIS, and Tafel polarization results, we conclude that the $La_2Mo_2O_7$/MWCNTs hybrids are potential catalysts for replacing Pt for future large-scale fabrication of DSSCs.

**Acknowledgements:** This work was financially supported by the National Natural Science Foundation of China (Grant No. 21473048 and 21303039), the Natural Science Foundation of Hebei Province (Grant No.B2015205163 and B2016205161), the Science and Technology Project of Hebei Province (No. 16211117) and the Natural Science Foundation of Hebei Education Department (Grant No.QN2017087).

## References:

[1] Armstrong G. *Nat. Chem.*, **2011**,**4**(1):4-5

[2] Hagfeldt A, Boschloo G, Sun L, et al. *Chem. Rev.*, **2010**,**110**(11):6595-6663

[3] Gonalves L M, Bermudez V D Z, Ribeiro H A, et al. *Energy Environ. Sci.*, **2008**,**1**(6):655-667

[4] ORegan B, Grtzel M. *Nature*, **1991**,**353**(6346):737-740

[5] Salam Z, Elayappan V, Angaiah S, et al. *Sol. Energy Mater. Sol. Cells.*, **2015**,**143**:250-259

[6] Shahzad N, Risplendi F, Pugliese D, et al. *J. Phys. Chem. C*, **2013**,**117**(44):22778-22783

[7] Polkoo S S, Saievar-Iranizad E, Bayatloo E. *Appl. Phys. A*, **2015**,**119**(4):1269-1276

[8] Wu M X, Lin Y N, Guo H Y, et al. *Nano Energy*, **2015**,**11**:540-549

[9] Wang L, Gao Z Y, Chang J L, et al. *ACS Appl. Mater. Interfaces*, **2015**,**7**(36):20234-20244

[10]Hsu Y C, Chen G L, Lee R H. *J. Polym. Res.*, **2014**,**21**(5):440 (9 Pages)

[11]Lowpa S, Samuk P, Maiaugree W, et al. *Mater. Lett.*, **2015**,**158**:115-118

[12]Towannang M, Kumlangwan P, Maiaugree W, et al. *Electron. Mater. Lett.*, **2015**,**11**(4):643-649

[13]Park K H, Kim S J, Gomes R, et al. *Chem. Eng. J.*, **2015**,**260**:393-398

[14]Al-bahrani M R, Xu X B, Ahmada W, et al. *Mater. Res. Bull.*, **2014**,**59**(59):272-277

[15]Tang Q W, Liu J, Zhang H H, et al. *J. Power Sources*, **2015**,**297**:1-8

[16]Tsai C H, Fei P H, Chen C H. *Materials*, **2015**,**8**:5715-5729

[17]Xia J, Yuan C, Yanagida S. *ACS Appl. Mater. Interfaces*, **2010**,**2**:2136-2139

[18]Wu M X, Guo H Y, Lin Y N, et al. *J. Phys. Chem. C*, **2014**,**118**(24):12625-12631

[19]Wu M X, Lin Y N, Guo H Y, et al. *Chem. Commun.*, **2014**,**50**(57):7625-7627

[20]Jia J B, Wu J H, Tu Y G, et al. *J. Alloys Compd.*, **2015**,**640**:29-33

[21]Mohamed I M A, Motlak M, Akhtar M S, et al. *Ceram. Int.*, **2016**,**42**(1):146-153

[22]Liu J, Tang Q W, He B L, et al. *J. Power Sources*, **2015**,**282**:79-86

[23]Jia J B, Wu J H, Tu Y G, et al. *J. Alloys Compd.*, **2015**,**640**:29-33

[24]Wu M X, Lin X, Hagfeldt A. *Chem. Commun.*, **2011**,**47**(15):4535-4537

[25]Gao C J, Han Q J, Wu M X. *J. Energy Chem.*, **2018**,**27**:703-712

[26]Chen S L, Tao J, Shu H B, et al. *J. Power Sources*, **2017**,**341**:60-67

[27]Zheng H K, Guo H Y, Wu K Z, et al. *J. Mater. Chem. C*, **2016**,**4**:6533-6538

[28]Xiong K W, Li G, Jin C, et al. *Mater. Lett.*, **2016**,**164**:609-612

[29]Areerob Y, Cho K Y, Oh W C. *J. Mater. Sci.-Mater. Electron.*, **2018**,**29**:3437-3438

[30]Mohammed J S. *A Study of High Temperature Reactions in Oxide-Dispersion-Strengthened Molybdenum at Reduced Oxygen Partial Pressure*. Georgia: Georgia Institute of Technology, **2004**:5

[31]Li Y Z, Jiang Y P, Wang T J, et al. *Sep. Purif. Technol.*, **2017**,**172**:415-421

[32]Chen S L, Tao J, Shu H B, et al. *J. Power Source*, **2017**,**341**:60-67

[33]Wu M X, Mu L, Wang Y D, et al. *J. Mater. Chem. A*, **2013**,**1**(25):7519-7524